Draft version May 16, 2022
Typeset using LaTeX **twocolumn** style in AASTeX63

Korg: a modern 1D LTE spectral synthesis package

Adam J. Wheeler,[1] Matthew W. Abruzzo,[1] Andrew R. Casey,[2,3] and Melissa K. Ness[1]

[1] *Department of Astronomy, Columbia University, Pupin Physics Laboratories, New York, NY 10027, USA*
[2] *School of Physics & Astronomy, Monash University, Victoria, Australia*
[3] *Center of Excellence for Astrophysics in Three Dimensions (ASTRO-3D)*

ABSTRACT

We present Korg, a new package for 1D LTE (local thermal equilibrium) spectral synthesis, which computes theoretical spectra from the near-ultraviolet to the near-infrared, and implements both plane-parallel and spherical radiative transfer. It is compatible with automatic differentiation libraries, and easily extensible, making it ideal for statistical inference and parameter estimation applied to large data sets. We outline the inputs and internals of Korg, and compare its output spectra to those produced by other codes. We use five example wavelength regions across 3660 Å – 15050 Å to show that the residuals between Korg and the other codes are no larger than that between existing codes themselves. We show that Korg is 1–100 times faster than other codes in typical use. Documentation and installation instructions are available at https://ajwheeler.github.io/Korg.jl/stable/.

Keywords: spectroscopy

1. INTRODUCTION

Improvements in instrumentation have yielded exponential growth in the amount of spectral data to analyse. Creating pipelines that can keep up with analysis is nontrivial. There are several extant codes for 1D LTE spectral synthesis, including Turbospectrum (Plez et al. 1993; Plez 2012), Moog (Sneden 1973; Sneden et al. 2012), SYNTHE (Kurucz 1993; Sbordone et al. 2004), SME, (Valenti & Piskunov 1996, 2012; Piskunov & Valenti 2017), and SPECTRUM (Gray & Corbally 1994). While they have enabled a huge volume of research, these codes can be difficult to use for the uninitiated, and require input and output through custom file formats, impeding integration into analysis code. Here we present Korg, a new 1D LTE synthesis package, written in Julia and suitable for easy integration with scripts and use in an interactive environment. As the first such code in more than two decades, Korg benefits from numerical libraries not available at the time earlier packages were authored.

Like most existing spectral synthesis packages, Korg simplifies analysis by assuming that atmospheres are in LTE—that baryonic matter is described by thermal distributions, and radiation is only very slightly out of equilibrium. The source function (the ratio of the per-volume emission and absorption coefficients) is dominated by collisions of baryonic matter and is Planckian. While non-LTE (NLTE) calculations are important for producing the most unbiased possible model spectra, they are prohibitively slow, and not yet suitable for application that require computing many spectra. Fortunately, corrections to LTE level populations (e.g. Amarsi et al. 2020), equivalent widths, or abundances (e.g. Lind et al. 2011; Amarsi et al. 2015; Bergemann et al. 2012; Osorio & Barklem 2016) can be calculated from NLTE simulations. These can be applied to LTE codes to produce approximate NLTE spectra at relatively little computational cost. Additionally, biases from the assumption of LTE will roughly cancel for similar stars, yielding differential abundance estimates with high precision.

The performance of spectral synthesis codes is most important when fitting observational data. Because synthesis must be embedded in an inference loop, the analysis of of a single spectrum may trigger tens or hundreds of syntheses. Even when many parameters may be estimated by interpolating over (or otherwise comparing to) a precomputed grid of spectra (e.g. Recio-Blanco et al. 2006; Smiljanic et al. 2014; Holtzman et al. 2018; Boeche et al. 2021; Buder et al. 2021), individual abundances are best done with targeted syntheses of individ-

Corresponding author: Adam Wheeler
a.wheeler@columbia.edu

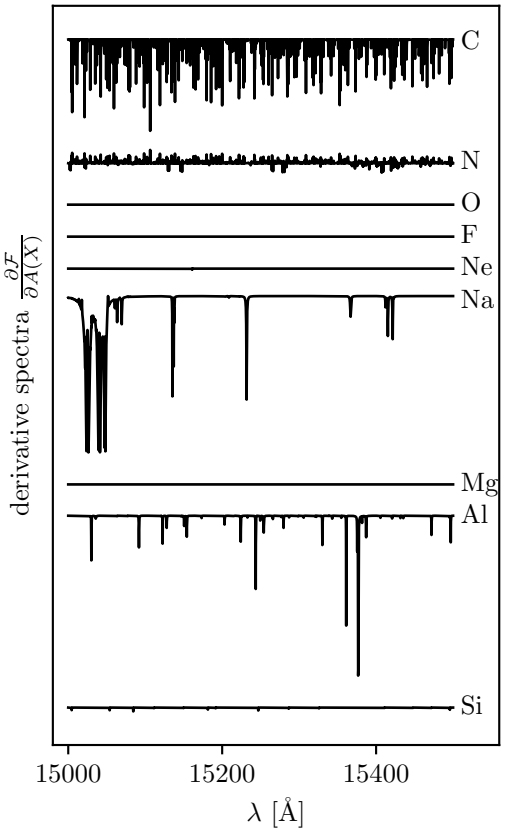

Figure 1. Derivatives of a synthesized solar spectrum with respect to various abundances, $\frac{\partial \mathcal{F}}{\partial A(X)}$. Vertical offsets have been applied, but the relative scaling is preserved, which is why some derivative spectra appear flat here (but show fluctuations at a sub-percent level).

ual lines. Furthermore, generating a grid from which to interpolate can be computationally expensive. Inference and optimization can also be sped up by fast and accurate derivatives of the function being sampled or minimized, most easily produced via automatic differentiation. Korg is designed to be compatible with automatic differentiation packages (e.g. ForwardDiff), which can provide derivative spectra in roughly the same amount of time required for a single synthesis (as discussed in Section 4; see Figure 1).

2. DESCRIPTION OF CODE

To synthesize a spectrum, Korg calculates the number density of each species (e.g. H I, C II, CO) at each layer in the atmosphere (Section 2.2), then computes the absorption coefficient at each wavelength and atmospheric layer due to continuum (Section 2.3) and line absorption (Section 2.4). Given the total absorption coefficient at each wavelength and atmospheric layer, it then solves the radiative transfer equation to produce the flux at the stellar surface (Section 2.5).

2.1. *Inputs*

Korg takes as inputs, a model atmosphere, a linelist, and abundances for each element in $A(X)$ form,[1] assumed to be constant throughout the atmosphere. By default, abundances follow the solar ratios from Asplund et al. (2009), and the abundances of elements can be set individually, or uniformly scaled with a `metallicity` parameter. Korg includes functions for parsing "mod"-format MARCS (Gustafsson et al. 2008) model atmospheres, and line lists in the format supplied by VALD (Piskunov et al. 1995; Kupka et al. 1999, 2000; Ryabchikova et al. 2015; Pakhomov et al. 2019) or Kurucz (Kurucz 2011), or those accepted by Moog. When parsing VALD linelists, Korg will automatically apply corrections to unscaled $\log(gf)$ values for transitions with isotope information using the isotopic abundance values supplied by Berglund & Wieser (2011). Korg detects and uses packed Anstee, Barklem, and O'Mara (ABO; Anstee & O'Mara 1991) if they are provided (as VALD optionally does). It uses vacuum wavelengths internally, and will automatically convert air-wavelength VALD linelists to vacuum (Birch & Downs 1994). Users may also construct line lists or model atmospheres using custom code and pass them directly into Korg.

2.2. *Chemical equilibrium*

In order to compute the absorption coefficient, α_λ, at each layer of the atmosphere, Korg must solve for the number density of each species. Treating the number density of each neutral atomic species as the free parameters, Korg uses the NLsolve library (Mogensen et al. 2020) to solve the system of Saha and molecular equilibrium equations with the temperature, total number density, and number density of free electrons set by the model atmosphere, and the total abundance of each element set by the user. By default, Korg uses atomic ionization energies, atomic partition functions, molecular equilibrium constants from Barklem & Collet (2016) (the ionization energies are originally from Haynes 2010), but alternatives can be passed by the user.

By default, Korg solves the equilibrium equations taking into account all elements up to uranium, as well as 247 diatomic molecules. As they exist in extremely small quantities in LTE atmospheres, Korg neglects species which are more than doubly ionized. It also ne-

[1] $A(X) = \log_{10}(n_X/n_\mathrm{H})+12$ where n_X is the total number density of element X and n_H that of hydrogen.

glects ionic and triatomic molecules at present, although we plan to address this in a future version.

2.3. *Continuum absorption*

KORG computes contributions to the continuum absorption coefficient from a number of sources, listed in Table 1. Continuum absorption mechanisms involving an atom and an electron can be classified as bound-free (bf) or free-free (ff), depending on whether the electron is initially bound to the atom. Note that these are named as though the electron were bound, even for free-free sources. For example, "H I bf" refers to the ionization of neutral hydrogen, and "H I ff" refers to absorption by the interaction of free electrons and free protons. See Table 1 for a list of included continuum absorption mechanisms. Gaunt factors for bf and ff absorption by hydrogenic atoms are taken from Karzas & Latter (1961) (via a polynomial fit in Kurucz 1970) and van Hoof et al. (2014), respectively. The contribution to the absorption coefficient from electron scattering, α_e, is calculated with the Thomson scattering cross section (Thomson 1912). At present, KORG treats all scattering as absorption, which is correct in the LTE regime. In the future we plan to support quasi-LTE radiative transfer with isotropic scattering, which will yield more accurate spectra when Rayleigh scattering dominates or is a significant source of opacity.

2.4. *Line absorption*

The contribution of each line to the total absorption coefficient, α_{line}, is

$$\alpha_\lambda^{\text{line}} = \sigma n \frac{\exp(-\beta E_{\text{up}}) - \exp(-\beta E_{\text{lo}})}{U(T)} \phi(\lambda) \tag{1}$$

where the wavelength-integrated cross-section, σ is given by

$$\sigma = g_{\text{lo}} f \frac{\pi e^2 \lambda_0^2}{m_e c^2} \quad . \tag{2}$$

Here, n is the number density of the line species, E_{up} and E_{lo} are the upper and lower energy levels of the transition, $\beta = 1/kT$ is the thermodynamic beta, ϕ is the normalized line profile, U is the species partition function, T is the temperature, f is the oscillator strength, g_{lo} is the degeneracy of the lower level, λ_0 is the line center, and m_e is the electron mass.

For all lines of all species besides hydrogen (including autoionizing lines), ϕ is approximated with a Voigt profile using the numerical approximation from Hunger (1956). The width of the Gaussian component is

$$\sigma_D = \lambda_0 \sqrt{\frac{2kT}{m} + \xi^2} \quad , \tag{3}$$

where m is the species mass, and ξ is the microturbulent velocity, a fudge factor used to account for convective Doppler-shifts. The width of the Lorentz component (in frequency rather than wavelength units) is given by

$$\Gamma = \Gamma_{\text{rad}} + \gamma_{\text{stark}} n_e + \gamma_{\text{vdW}} n_{\text{H I}} \quad , \tag{4}$$

where Γ_{rad} is the radiative broadening parameter, γ_{stark} the per-electron Stark broadening parameter, γ_{vdW} the per-neutral-hydrogen van der Waals broadening parameter, and n_e and $n_{\text{H I}}$ are the number densities of free electrons and neutral hydrogen, respectively. We neglect pressure broadening of molecular lines, setting γ_{stark} and γ_{vdW} to zero.

When Γ_{rad} is not supplied in the linelist, KORG approximates it with

$$\Gamma_{\text{rad}} = \frac{8\pi^2 e^2}{mc\lambda^2} gf \quad , \tag{5}$$

where m is the mass of the atom or molecule, g is the degeneracy of the lower level of the transition, and f is the transition oscillator strength. This can be obtained by assuming that spontaneous de-exitation dominates the transition's energy uncertainty, and that the upper level's degeneracy is unity.

The values of γ_{stark} and γ_{vdW} at 10^5 K, γ_0^{stark} and γ_0^{vdW}, are provided by the linelist, then scaled by their temperature dependence according to semiclassical impact theory (e.g. Hubeny & Mihalas 2014 ch. 8.3) to the per-particle broadening parameters:

$$\gamma_{\text{stark}} = \gamma_0^{\text{stark}} \left(\frac{T}{10^5 \text{ K}} \right)^{\frac{1}{6}} \tag{6}$$

$$\gamma_{\text{vdW}} = \gamma_0^{\text{vdW}} \left(\frac{T}{10^5 \text{ K}} \right)^{\frac{3}{10}} \tag{7}$$

If provided, ABO parameters, which describe a more nuanced temperature dependence in broadening by neutral hydrogen, will be used to calculate γ_{vdW} instead. When a Stark broadening parameter is not provided in the linelist, the approximation from Cowley (1971) is used. When a van der Waals broadening parameter is provided, a form of the the Unsöld approximation (Unsold 1955; Warner 1967) is used in which the angular momentum quantum number is neglected and the mean square radius, $\overline{r^2}$, is approximated by

$$\overline{r^2} = \frac{5}{2} \left(\frac{{n_{\text{eff}}}^2}{Z} \right)^2 \quad , \tag{8}$$

where n_{eff} is the effective principal quantum number and Z is the atomic number. Pressure broadening is neglected for autoionizing lines with no provided parameters.

Absorption source	Wavelength bounds	Temperature bounds	Reference
H I bf			Kurucz (1970)
H I ff	100 Å – 10^6 Å	100 K – 10^6 K	van Hoof et al. (2014)
H^- bf	$\geq$ 1250 Å		Wishart (1979)*
H^- ff	2604 Å – 113,918 Å	2520 K – 10,080 K	Bell & Berrington (1987)*
H_2^+ bf and ff	700 Å – 20,000 Å	3150 K – 25,200 K	Stancil (1994)
He II bf			Kurucz (1970)
He II ff	100 Å – 10^6 Å	100 K – 10^6 K	van Hoof et al. (2014)
He^- ff	5063 Å – 151,878 Å	2520 K – 10,080 K	John (1994)*
H Rayleigh	$\geq$ 1300 Å		Lee (2005)†
He Rayleigh	$\geq$ 1300 Å		Dalgarno & Kingston (1960); Dalgarno (1962); Schwerdtfeger (2006)†
H_2 Rayleigh	$\geq$ 1300 Å		Dalgarno & Williams (1962)
electron scattering			Thomson (1912)

Table 1. Sources of continuum absorption in KORG. References marked with "*" are via polynomial fits in Gray (2005). Those marked with "†" are via Colgan et al. (2016). When bounds in temperature or wavelength are missing, the absorption coefficient is defined for all positive values.

The absorption coefficient for each line (except those of hydrogen) is calculated over a dynamically determined wavelength range. The maximum detuning (wavelength difference from the line center) is set to the value at which a pure Gaussian or pure Lorentzian profile takes on a value of $\alpha_{\rm crit}$, whichever is larger. By default, KORG truncates profiles at $\alpha_{\rm crit} = 10^{-3}\alpha_{\rm cntm}$, where $\alpha_{\rm cntm}$ is the local continuum absorption coefficient. This ratio, $\alpha_{\rm crit}/\alpha_{\rm cntm}$, can be set by the user.

The broadening of hydrogen lines is treated separately. We use the tabulated Stark broadening profiles from (Stehlé & Hutcheon 1999), which are pre-convolved with Doppler profiles. For H_α, H_β, and H_γ, where self-broadening is important, we add to ϕ a Voigt profile using the p-d approximation for self-broadening from Barklem et al. (2000).

2.5. *Radiative transfer*

KORG solves the radiative transfer equation in a plane-parallel atmosphere,

$$\frac{\mu}{\alpha_\lambda}\frac{\mathrm{d}I_\lambda}{\mathrm{d}z} = S_\lambda - I_\lambda \quad , \tag{9}$$

or in a spherical atmosphere,

$$\frac{\mu}{\alpha_\lambda}\frac{\partial I_\lambda}{\partial r} + \frac{1-\mu^2}{\alpha_\lambda r}\frac{\partial I_\lambda}{\partial \mu} = S_\lambda - I_\lambda \quad , \tag{10}$$

where I_λ is the intensity of radiation at wavelength λ, S_λ the source function, α_λ the absorption coefficient, z the negative depth into the atmosphere, r, the distance to the center of the star, and μ the cosine of the angle between the r/z axis and the line of sight. When the thickness of the atmosphere is small relative to the stellar radius, curvature can be neglected and a plane-parallel atmosphere is a good approximation, otherwise sphericity must be taken into account. By default, KORG does it's radiative transfer calculations in the same geometry as the model atmosphere.

What KORG actually returns is the disk-averaged intensity, i.e. the astrophysical flux,

$$\mathcal{F}_\lambda = 2\pi \int_0^1 \mu I_\lambda^{\rm top}(\mu)\,\mathrm{d}\mu \quad . \tag{11}$$

Here, $I_\lambda^{\rm top}(\mu)$ stands for $I_\lambda(z=0,\mu)$ in the plane-parallel case and $I_\lambda(r=R,\mu)$ in the spherical case, where R is the radius of the outermost atmospheric layer. The total flux from the star is then $F_\lambda = (R/d)^2\mathcal{F}_\lambda$, where d is the distance to the star. Since KORG assumes that the stellar atmosphere is in LTE, S_λ is the blackbody spectrum.

In the plane-parallel case,

$$\mathcal{F}_\lambda = 2\pi \int_{\tau'_\lambda}^0 S_\lambda(\tau_\lambda)E_2(\tau_\lambda)\mathrm{d}\tau_\lambda \quad , \tag{12}$$

where E_2 is the second order exponential integral, τ_λ is the optical depth ($\mathrm{d}\tau_\lambda = \alpha_\lambda \mathrm{d}z$) and τ'_λ is the depth at the bottom of the atmosphere. The spherical case admits no further analytic simplifications. When using a spherical model atmosphere, to obtain the astrophysical flux, $\mathcal{F}_\lambda$, KORG calculates the intensity, $I_\lambda^{\rm top}$ at a discrete grid of μ values, by integrating along rays from the lowest atmospheric layer to the top atmospheric layer for many of surface μ values. This is valid since the source function is isotropic under LTE. Rays which do not intersect the lowest atmospheric layer are cast from the far side of the star.

Regardless of the atmosphere geometry, KORG scales its absorption coefficients so that the continuum absorp-

tion at the reference wavelength (5000 Å) matches that in the model atmosphere. Appendix A contains a few numerical details on the calculation of transfer integrals.

3. SCIENTIFIC VERIFICATION

To test Korg's correctness, we compare its spectra to those produced by Moog and Turbospectrum for the parameters ($T_{\rm eff}$, $\log g$, and metallicity) of four stars: the Sun, Arcturus, HD122563 (an extremely metal-poor red giant), and HD49933 (an F-type main sequence star). For all stars, the solar abundance pattern was assumed, which is not problematic since we are comparing synthetic spectra to each other and not to observational data. Figures 2 – 5 show these comparisons in six (vacuum) wavelength regions:

- 3660 Å – 3670 Å, near the Balmer jump
- 3935 Å – 3948 Å, in the wing of the Ca II Fraunhofer K line
- 5160 Å – 5175 Å, including two lines of the Fraunhofer b Mg triplet
- 6540 Å – 6580 Å, including H_α
- 15000 Å – 15050 Å, in the near-infrared, part of the APOGEE wavelength region
- The continuum across 2000Å – 10000 Å, computed without any lines

For the first four regions, we used an "extract all" linelist from VALD, which includes all known lines within the wavelength bounds. The near-infrared spectrum was synthesized using the APOGEE DR16 linelist (Jönsson et al. 2020). As Moog can handle a limited number of lines within the opacity contribution window (typically 2 Å), we culled the weakest TiO lines from each list, reducing the total number of transitions passed to Moog to be at most 10,000. Additionally, as Moog lacks a special treatment for hydrogen lines, we omitted these from its linelist. Since Korg (see Section 2.3) and Moog (excepting the fork presented in Sobeck et al. 2011) do not support true scattering, we set the `PURE-LTE` flag to true in `babsma.par`, setting Turbospectrum to turn off this functionality. There is good agreement between the codes. In the following subsections, we enumerate and discuss the notable discrepancies.

3.1. *Continuum absorption in the violet and ultraviolet*

Near the Balmer jump and blueward, the Korg and Moog continua diverge from the Turbospectrum continuum. This is the primary cause for the disagreement between the codes in the first two wavelength regions, which are in the region where the continua disagree. The discrepancy most likely arises from Korg's lack of continuum absorption from metals. We anticipate that future versions of Korg incorporating more continuum absorption mechanisms will predict continua closer to those predicted by Turbospectrum.

3.2. *Balmer series*

There is minor disagreement between Korg and Turbospectrum at H_α (the fourth wavelength region). Turbospectrum predicts slightly stronger absorption in the wings of the line (see particularly HD49933, Figure 4). For HD122563, there is also strong disagreement between Korg and Turbospectrum at the H_α core. Given that accurate modelling of H_α requires techniques beyond 1D LTE (e.g. Barklem 2007; Amarsi et al. 2018), this disagreement is permissible.

There are eight Balmer series lines in the 3660 Å– 3670 Å(vacuum) wavelength region (upper levels $n = 26$ to $n = 33$), five of which are included in Korg (those up to $n = 30$). Typically, these have a very minimal impact on the observed spectrum, but in HD122563 Korg predicts that these lines are visible as broad shallow features, in contrast to Turbospectrum (hydrogen lines are omitted from the Moog linelist). They are located at 3668.76 Å, 3667.17 Å, 3665.75 Å, 3664.48 Å, and 3663.33 Å (vacuum), and are more clearly visible in the residuals panel. A possible explanation for the disagreement is that Turbospectrum's hydrogen line prescription may not extend to energy levels this high. In high-resolution ultraviolet spectra of HD122563[2], the lines are present, so we conclude that the disagreement doesn't indicate a problem in Korg.

3.3. *C_2 band*

Korg predicts stronger absorption by the C_2 band from roughly 5160 Å – 5165 Å than the other two codes. This is because the codes use different prescriptions for the molecular equilibrium constants, $K_{C_2}(T)$. Based on logging information, Turbospectrum appears to use the polynomial expansions from Tsuji (1973). We weren't able to determine the source of the prescriptions used by Moog, but we were able to extract the polynomial approximation for the C_2 molecular equilibrium constant from the source code. We compared both approximations to the Barklem & Collet (2016) values and

[2] e.g. this spectum (archive ID: ADP.2021-08-26T17:20:56.312) taken by the Ultraviolet and Visual Echelle Spectrograph at the Very Large Telescope (Dekker et al. 2000).

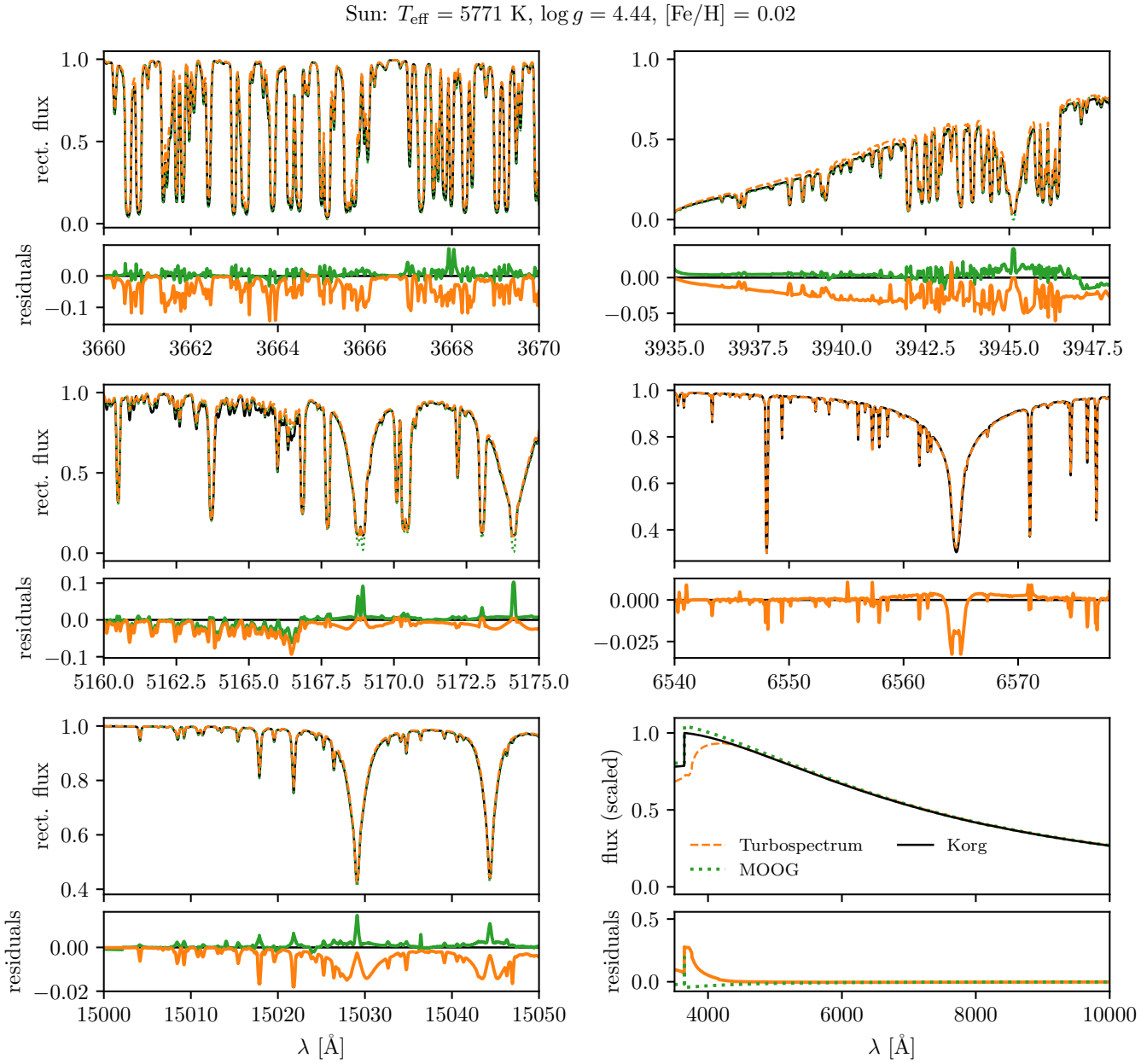

Figure 2. Portions of a synthetic solar spectrum generated with Korg, Moog, and Turbospectrum, as well as the continuum generated with an empty linelist from 4000 Å to 10000 Å. All wavelengths are vacuum. The residuals (Korg - other) are shown underneath the rectified flux for each wavelength region. The level of agreement between Korg and the other codes is similar to their agreement with each other. See text for a discussion of the discrepancies.

found that they will predict C_2 number densities which are 40% - 80% of the Korg values in the Sun. The discrepancy is likely due in large part to the use of different values for the dissolution energy of C_2 (see discussion in Barklem & Collet 2016). This accounts precisely for the discrepancy in C_2 number density through the atmosphere between Moog and Korg. We were not able to extract number densities from Turbospectrum, but the fact that it predicts slightly less C_2 absorption than Moog is consistent with its slightly higher values of K_{C_2}.

4. BENCHMARKS

Figure 6 shows the time taken by of Korg, Turbospectrum, and Moog to produce the spectra in Section 3. All test are single-core, and run on the same machine with an AMD Epyc 7702P. The infrared region was extended to 15000 Å – 15500 Å to provide a example synthesis over a larger wavelength region. This region,

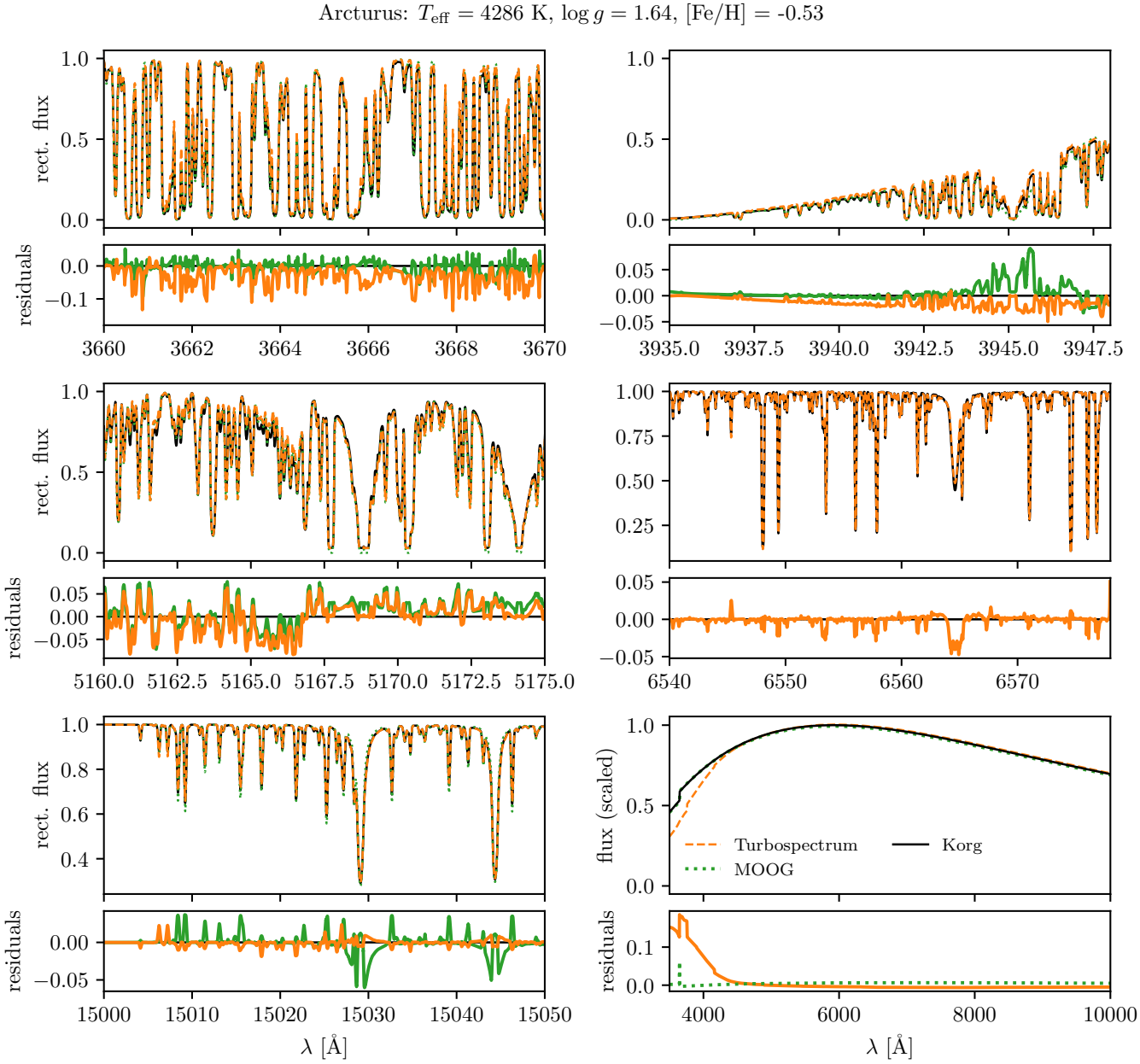

Figure 3. Same as Figure 2, but showing the synthetic spectrum of Arcturus.

synthesized with the APOGEE DR16 linelist, provides a realistic example of synthesizing a spectrum from a large "industrial" survey. The others, which used VALD "extract all" linelists, include more lines than would typically be used, including many which have essentially no effect on the spectrum.

KORG only need to load linelists and model atmosphere into memory once, so repeat syntheses which use the same inputs (as would be the case when varying individual abundances) avoid that step. For these comparisons, loading the linelist ($10^5 - 10^6$ transitions) takes 1 – 4 seconds, and loading the model atmosphere takes roughly 0.05 ms. As nearly all cases in which performance required involve repeated synthesizing with the same (or nearly the same) linelist, we did not optimize input parsing for speed and do not include this time in KORG benchmarks. We note also that the MOOG values should be taken as a lower limit, since the linelists provided to MOOG were reduced in size by an order of magnitude or more. Figure 6 has separate markers for TURBOSPECTRUM with and without hydrogen lines, as we found them to slow down synthesis by a very large factor. In wavelength ranges where hydrogen lines are

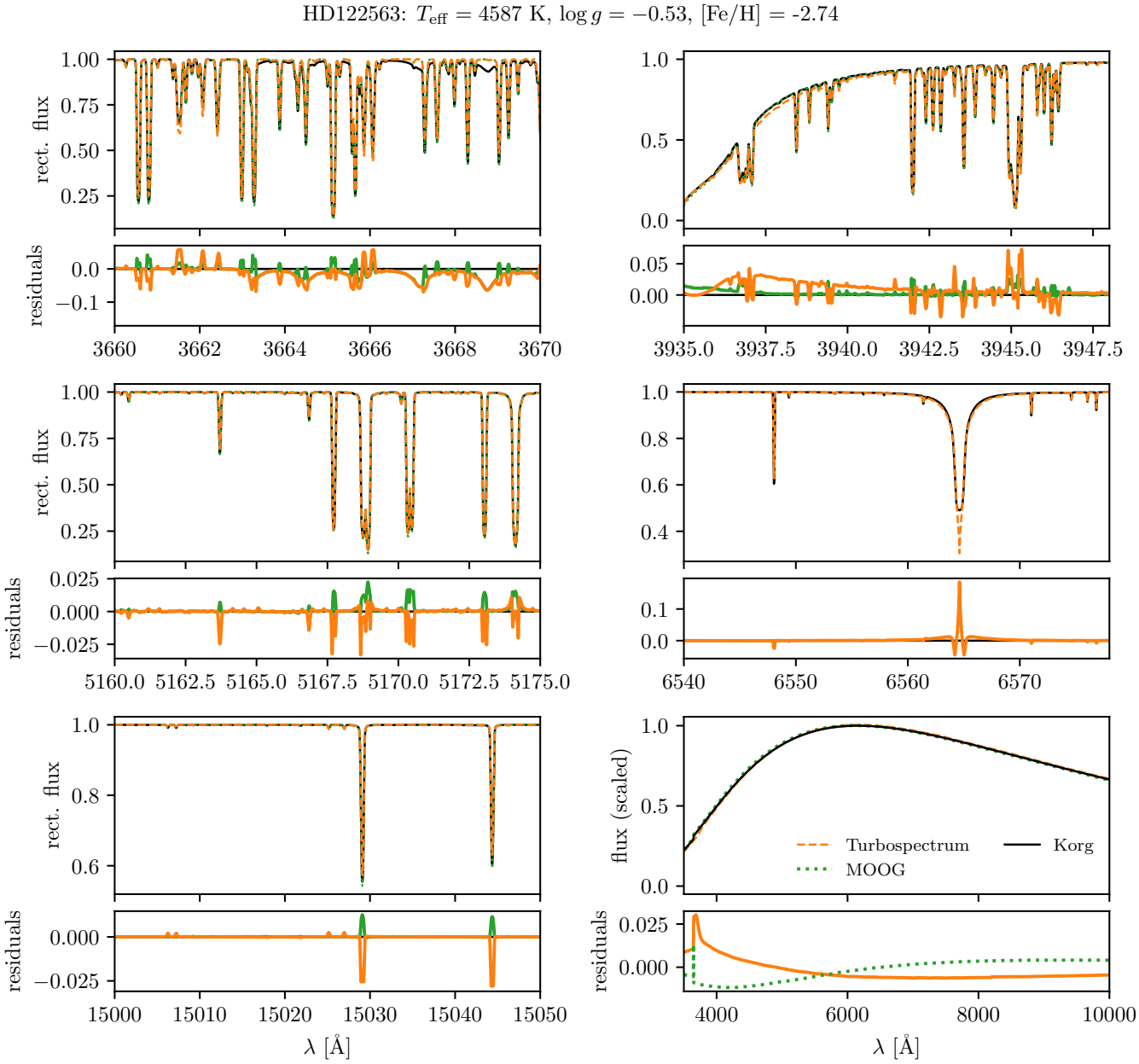

Figure 4. Same as Figure 2, but showing the synthetic spectrum of HD122563.

not present or unimportant, they can be omitted, and TURBOSPECTRUM executes much more quickly.

In the top panel of Figure 7 we plot the time required by KORG to compute the gradient of the solar spectrum, $\frac{\partial \mathcal{F}}{\partial A(X)}$, with regard to a varying numbers of element abundances, N. (See Figure 1 for a subset of the derivative spectra.) For this demonstration we used the 15,000 – 15,500 Å range and the APOGEE DR16 linelist. A dashed horizontal line marks the time required to synthesize the spectrum, just under one second. Calculating the N-dimensional gradient spectrum takes roughly $2 + 0.15N$ seconds, meaning that the marginal time required for each derivative is an order of magnitude smaller than the time required to obtain it via finite differences. As JULIA's automatic differentiation ecosystem improves, KORG may benefit from further speedups to the calculation of gradient spectra. Calculating derivative spectra with respect to atmospheric parameters, e.g. $T_{\rm eff}$, $\log g$, or $v_{\rm mic}$, requires code to interpolate between model atmospheres, which we plan to add to KORG.

5. CONCLUSIONS

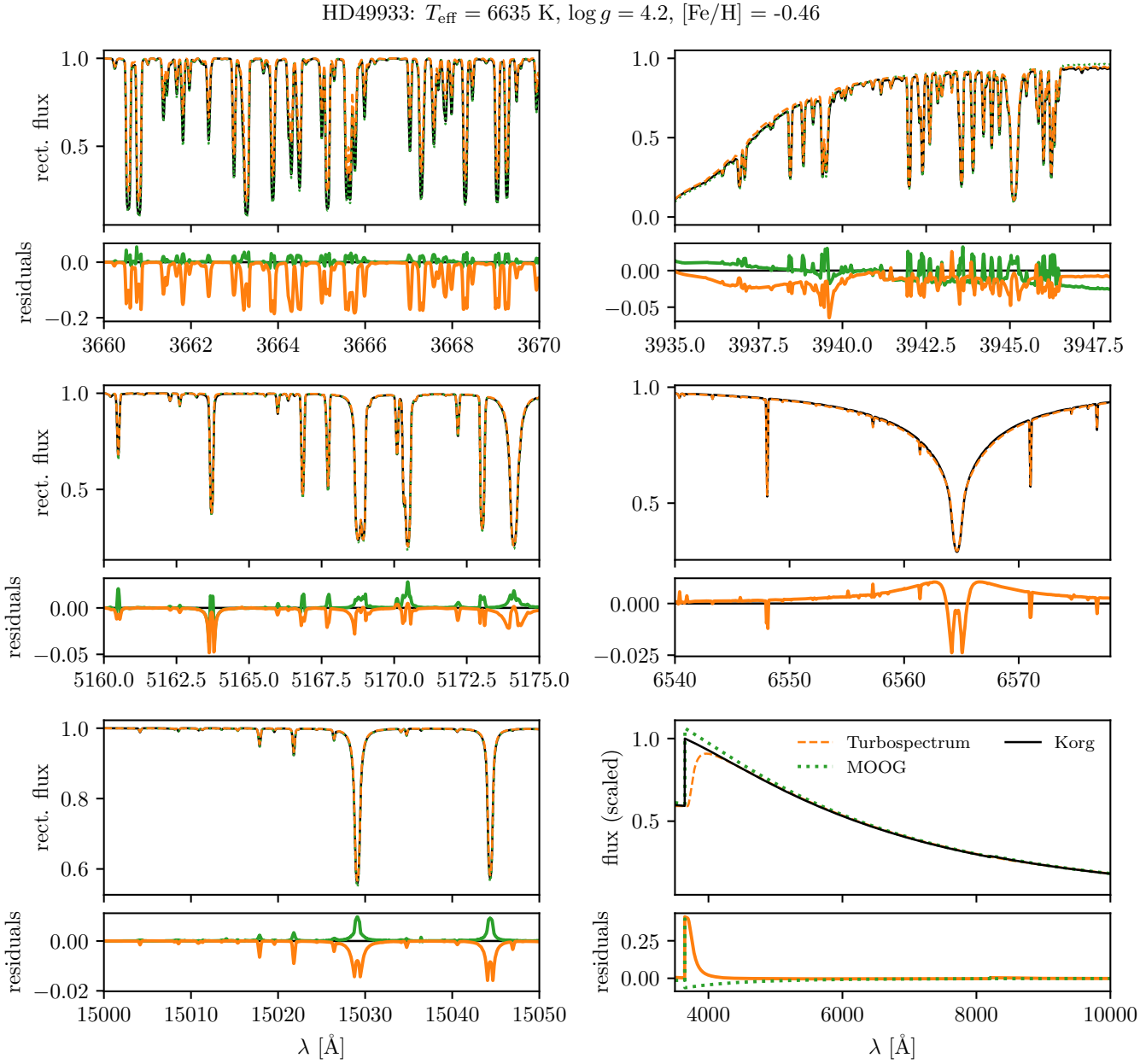

Figure 5. Same as Figure 2, but showing the synthetic spectrum of HD49933.

We have presented a new code, KORG, for 1D LTE spectral synthesis, i.e. computing stellar spectra given a model atmosphere, linelist, and element abundances. The code is publicly available at https://github.com/ajwheeler/Korg.jl and installable via the JULIA package manager. Detailed documentation, usage examples (including the use of FORWARDDIFF (Revels et al. 2016) to compute derivatives of the spectrum with regard to input parameters) , and installation instructions are available at https://ajwheeler.github.io/Korg.jl/stable.

We are aware of two current limitations which are worth highlighting. First, support for metal absorption coefficients in KORG is still experimental and not exposed in the public interface, so caution is warranted in the ultraviolet. Note, though, that agreement with MOOG is good in the very-near ultraviolet (below 3600 Å – 3800 Å), and that MOOG and TURBOSPECTRUM disagree significantly in the ultraviolet. Second, we note that the KORG's built-in partition functions (from Barklem & Collet 2016) are defined only up to 10,000 K, meaning that stars with significant portions of the atmosphere hotter than 10,000 K are not well-modelled without user-supplied partition functions.

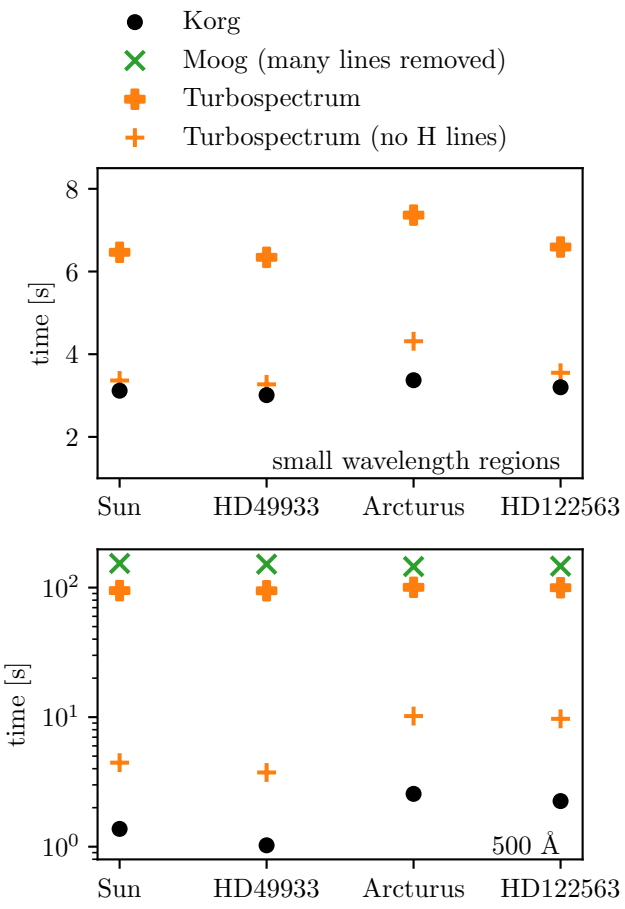

Figure 6. The time taken by KORG, MOOG, and TURBOSPECTRUM for the syntheses in Section 3. **top:** average compute time for the optical wavelength regions, which used very dense linelists. **bottom:** compute time to synthesize spectra from 15,000 – 15,500 Å with the APOGEE DR16 linelist, a more "realistic" use case. Note that the wavelength regions synthesized were larger than those plotted in Figures 2 – 5.

Aside from these highlighted limitations and the lack of true scattering (mentioned in Section 2.3)), KORG has a few additional limitations that we plan to eliminate in the near future. As mentioned in Section 4, calculating derivative spectra with regard to atmospheric parameters like $\log g$ or $T_{\rm eff}$, requires code to interpolate model atmospheres which is written in JULIA. Relatedly, while inferring stellar abundances and parameters with KORG is not overly burdensome, the user must still apply the line spread function to synthesized spectra and calculated goodness-of-fit themselves, processes we would like to automate. Lastly, support for triatomic molecules in KORG is required to support the modelling of H_2O and CO_2.

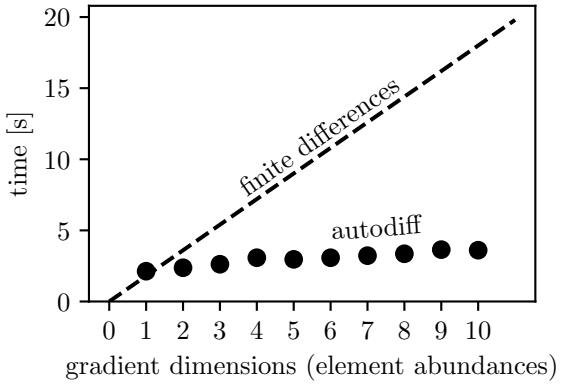

Figure 7. top: Time required to compute simultaneous derivative of spectrum with regard to N different element abundances, for varying N.

Our goal is that KORG will be useful for both inference of stellar parameters and abundances for large survey data, e.g. *Gaia* (Gaia Collaboration et al. 2016), SDSS-V (Kollmeier et al. 2017), MOONS (Kollmeier et al. 2017), WEAVE Dalton et al. (2012), 4-MOST (de Jong et al. 2019), LAMOST (Deng et al. 2012; Zhao et al. 2012), GALAH (De Silva et al. 2015), and for boutique analyses of individual spectra. We aim to make KORG fast and flexible enough to enable better survey pipelines and novel analyses, such as the propagation of error from synthesis inputs to synthesized spectra, or the joint inference of line parameters with observational data. In addition, we hope that by making KORG as easy to use as possible, more researchers will find it worthwhile to synthesize spectra when the need arises.

ACKNOWLEDGMENTS

AJW would like to thank Chris Sneden for his advice, Samuel Potter, Paul Barklem, Karen Lind, and Thomas Nordlander for answers to naive questions, and Rob Rutten, David F. Gray, Ivan Hubeny, Robert Kurucz, and Dimitri Mihalas for writing excellent reference material. He would also like to thank Charlie Conroy for his interest and encouragement, and David Hogg for putting him in touch with Mike O'Neil and Samuel Potter.

AJW is supported by the National Science Foundation Graduate Research Fellowship under Grant No. 1644869. MKN is in part supported by a Sloan Research Fellowship. A. R. C. is supported in part by the Australian Research Council through a Discovery Early Career Researcher Award (DE190100656). Parts of this research were supported by the Australian Research Council Centre of Excellence for All Sky Astrophysics in 3 Dimensions (ASTRO 3D), through project number CE170100013.

This research has made use of the services of the ESO Science Archive Facility. Based on observations collected at the European Southern Observatory under ESO programme 266.D-5655. This work has made use of the VALD database, operated at Uppsala University, the Institute of Astronomy RAS in Moscow, and the University of Vienna.

REFERENCES

Amarsi, A. M., Asplund, M., Collet, R., & Leenaarts, J. 2015, Mon. Not. R. Astron. Soc., 454, L11, doi: 10.1093/mnrasl/slv122

Amarsi, A. M., Nordlander, T., Barklem, P. S., et al. 2018, Astron. Astrophys., 615, A139, doi: 10.1051/0004-6361/201732546

Amarsi, A. M., Lind, K., Osorio, Y., et al. 2020, Astron. Astrophys., 642, A62, doi: 10.1051/0004-6361/202038650

Anstee, S. D., & O'Mara, B. J. 1991, Monthly Notices of the Royal Astronomical Society, 253, 549, doi: 10.1093/mnras/253.3.549

Asplund, M., Grevesse, N., Sauval, A. J., & Scott, P. 2009, Annu. Rev. Astron. Amp Astrophys. Vol 47 Issue 1 Pp481-522, 47, 481, doi: 10.1146/annurev.astro.46.060407.145222

Barklem, P. S. 2007, Astron. Astrophys., 466, 327, doi: 10.1051/0004-6361:20066686

Barklem, P. S., & Collet, R. 2016, Astron. Astrophys., 588, A96, doi: 10.1051/0004-6361/201526961

Barklem, P. S., Piskunov, N., & O'Mara, B. J. 2000, ArXivastro-Ph0010022. https://arxiv.org/abs/astro-ph/0010022

Bell, K. L., & Berrington, K. A. 1987, J. Phys. B At. Mol. Phys., 20, 801, doi: 10.1088/0022-3700/20/4/019

Bergemann, M., Hansen, C. J., Bautista, M., & Ruchti, G. 2012, Astron. Astrophys., 546, A90, doi: 10.1051/0004-6361/201219406

Berglund, M., & Wieser, M. E. 2011, Pure Appl. Chem., 83, 397, doi: 10.1351/PAC-REP-10-06-02

Birch, K. P., & Downs, M. J. 1994, Metrologia, 31, 315, doi: 10.1088/0026-1394/31/4/006

Boeche, C., Vallenari, A., & Lucatello, S. 2021, Astron. Astrophys., 645, A35, doi: 10.1051/0004-6361/202038973

Buder, S., Sharma, S., Kos, J., et al. 2021, Mon. Not. R. Astron. Soc., 506, 150, doi: 10.1093/mnras/stab1242

Colgan, J., Kilcrease, D. P., Magee, N. H., et al. 2016, Astrophys. J., 817, 116, doi: 10.3847/0004-637X/817/2/116

Cowley, C. R. 1971, The Observatory, 91, 139

Dalgarno, A. 1962, Spectral Reflectivity of the Earth's Atmosphere III: The Scattering of Light by Atomic Systems, Tech. Rep. 62-20-A, Geophysical Corporation of America

Dalgarno, A., & Kingston, A. E. 1960, Proc. R. Soc. Lond. Ser. A, 259, 424, doi: 10.1098/rspa.1960.0237

Dalgarno, A., & Williams, D. A. 1962, Astrophys. J., 136, 690, doi: 10.1086/147428

Dalton, G., Trager, S. C., Abrams, D. C., et al. 2012, 8446, 84460P, doi: 10.1117/12.925950

de Jong, R. S., Agertz, O., Berbel, A. A., et al. 2019, The Messenger, 175, 3, doi: 10.18727/0722-6691/5117

De Silva, G. M., Freeman, K. C., Bland-Hawthorn, J., et al. 2015, Monthly Notices of the Royal Astronomical Society, 449, 2604, doi: 10.1093/mnras/stv327

Dekker, H., D'Odorico, S., Kaufer, A., Delabre, B., & Kotzlowski, H. 2000, 4008, 534, doi: 10.1117/12.395512

Deng, L.-C., Newberg, H. J., Liu, C., et al. 2012, Res. Astron. Astrophys., 12, 735, doi: 10.1088/1674-4527/12/7/003

Gaia Collaboration, Prusti, T., de Bruijne, J. H. J., et al. 2016, Astronomy and Astrophysics, 595, A1, doi: 10.1051/0004-6361/201629272

Gray, D. F. 2005, The Observation and Analysis of Stellar Photospheres

Gray, R. O., & Corbally, C. J. 1994, The Astronomical Journal, 107, 742, doi: 10.1086/116893

Gustafsson, B., Edvardsson, B., Eriksson, K., et al. 2008, Astron. Astrophys., 486, 951, doi: 10.1051/0004-6361:200809724

Haynes, W. M., ed. 2010, CRC Handbook of Chemistry and Physics, 91st Edition, 91st edn. (Boca Raton, Fla.: CRC Press)

Holtzman, J. A., Hasselquist, S., Shetrone, M., et al. 2018, AJ, 156, 125, doi: 10.3847/1538-3881/aad4f9

Hubeny, I., & Mihalas, D. 2014, Theory of Stellar Atmospheres

Hunger, K. 1956, Z. Astrophys., 39, 36

John, T. L. 1994, Mon. Not. R. Astron. Soc., 269, 871, doi: 10.1093/mnras/269.4.871

Jönsson, H., Holtzman, J. A., Allende Prieto, C., et al. 2020, Astron. J., 160, 120, doi: 10.3847/1538-3881/aba592

Karzas, W. J., & Latter, R. 1961, Astrophys. J. Suppl. Ser., 6, 167, doi: 10.1086/190063

Kollmeier, J. A., Zasowski, G., Rix, H.-W., et al. 2017, arXiv e-prints, 1711, arXiv:1711.03234

Kupka, F., Piskunov, N., Ryabchikova, T. A., Stempels, H. C., & Weiss, W. W. 1999, Astron. Astrophys. Suppl. Ser., 138, 119, doi: 10.1051/aas:1999267

Kupka, F. G., Ryabchikova, T. A., Piskunov, N. E., Stempels, H. C., & Weiss, W. W. 2000, Balt. Astron., 9, 590, doi: 10.1515/astro-2000-0420

Kurucz, R. L. 1970, SAO Spec. Rep., 309

—. 1993, Kurucz CD-ROM, Cambridge, MA: Smithsonian Astrophysical Observatory, —c1993, December 4, 1993

—. 2011, Can. J. Phys., 89, 417, doi: 10.1139/p10-104

Lee, H.-W. 2005, Mon. Not. R. Astron. Soc., 358, 1472, doi: 10.1111/j.1365-2966.2005.08859.x

Lind, K., Asplund, M., Barklem, P. S., & Belyaev, A. K. 2011, Astron. Astrophys., 528, A103, doi: 10.1051/0004-6361/201016095

Mogensen, P. K., Carlsson, K., Villemot, S., et al. 2020, JuliaNLSolvers/NLsolve.Jl: V4.5.1, Zenodo, doi: 10.5281/zenodo.4404703

Osorio, Y., & Barklem, P. S. 2016, Astron. Astrophys., 586, A120, doi: 10.1051/0004-6361/201526958

Pakhomov, Y. V., Ryabchikova, T. A., & Piskunov, N. E. 2019, Astron. Rep., 63, 1010, doi: 10.1134/S1063772919120047

Piskunov, N., & Valenti, J. A. 2017, A&A, 597, A16, doi: 10.1051/0004-6361/201629124

Piskunov, N. E., Kupka, F., Ryabchikova, T. A., Weiss, W. W., & Jeffery, C. S. 1995, Astron. Astrophys. Suppl. Ser., 112, 525

Plez, B. 2012, Astrophysics Source Code Library, ascl:1205.004

Plez, B., Smith, V. V., & Lambert, D. L. 1993, The Astrophysical Journal, 418, 812, doi: 10.1086/173438

Recio-Blanco, A., Bijaoui, A., & De Laverny, P. 2006, Monthly Notices of the Royal Astronomical Society, 370, 141, doi: 10.1111/j.1365-2966.2006.10455.x

Revels, J., Lubin, M., & Papamarkou, T. 2016, Forward-Mode Automatic Differentiation in Julia

Ryabchikova, T., Piskunov, N., Kurucz, R. L., et al. 2015, Phys. Scr., 90, 054005, doi: 10.1088/0031-8949/90/5/054005

Sbordone, L., Bonifacio, P., Castelli, F., & Kurucz, R. L. 2004, Memorie della Societa Astronomica Italiana Supplementi, 5, 93

Schwerdtfeger, P. 2006, in Computational, Numerical and Mathematical Methods in Sciences and Engineering, Vol. Volume 1, Atoms, Molecules and Clusters in Electric Fields (PUBLISHED BY IMPERIAL COLLEGE PRESS AND DISTRIBUTED BY WORLD SCIENTIFIC PUBLISHING CO.), 1–32, doi: 10.1142/9781860948862_0001

Smiljanic, R., Korn, A. J., Bergemann, M., et al. 2014, Astron. Astrophys., 570, A122, doi: 10.1051/0004-6361/201423937

Sneden, C. 1973, Astrophys. J., 184, 839, doi: 10.1086/152374

Sneden, C., Bean, J., Ivans, I., Lucatello, S., & Sobeck, J. 2012, Astrophysics Source Code Library, ascl:1202.009

Sobeck, J. S., Kraft, R. P., Sneden, C., et al. 2011, Astron. J., 141, 175, doi: 10.1088/0004-6256/141/6/175

Stancil, P. C. 1994, Astrophys. J., 430, 360, doi: 10.1086/174411

Stehlé, C., & Hutcheon, R. 1999, Astron. Astrophys. Suppl. Ser., 140, 93, doi: 10.1051/aas:1999118

Thomson, S. J. J. 1912, Lond. Edinb. Dublin Philos. Mag. J. Sci., doi: 10.1080/14786440408637241

Tsuji, T. 1973, Astron. Astrophys. Vol 23 P 411 1973, 23, 411

Unsold, A. 1955, Physik Der Sternatmospharen, MIT Besonderer Berucksichtigung Der Sonne.

Valenti, J. A., & Piskunov, N. 1996, Astronomy and Astrophysics Supplement Series, 118, 595

—. 2012, Astrophysics Source Code Library, ascl:1202.013

van Hoof, P. A. M., Williams, R. J. R., Volk, K., et al. 2014, Mon. Not. R. Astron. Soc., 444, 420, doi: 10.1093/mnras/stu1438

Warner, B. 1967, . ., 136, 8

Wishart, A. W. 1979, Mon. Not. R. Astron. Soc., 187, 59P, doi: 10.1093/mnras/187.1.59P

Zhao, G., Zhao, Y., Chu, Y., Jing, Y., & Deng, L. 2012, ArXiv12063569 Astro-Ph. https://arxiv.org/abs/1206.3569

APPENDIX

A. NUMERICAL EVALUATION OF TRANSFER INTEGRALS

To solve the equation of radiative transfer along a ray, KORG approximates the source function, S (λ subscripts dropped for brevity), with linear interpolation over optical depth, τ. Between each adjacent pair of atmospheric layers, we have $S(\tau) \approx m\tau + b$, so the (indefinite) transfer integral has solution

$$\int (m\tau - b)\exp(-\tau)\mathrm{d}\tau = -\exp(-\tau)\left(b + m(\tau + 1)\right) \quad . \tag{A1}$$

When evaluating equation 12, KORG uses the same approximation,

$$\int (m\tau - b)E_2(\tau)\mathrm{d}\tau = \frac{1}{6}\left[\tau E_2(\tau)(3b + 2m\tau) - \exp(\tau)(3b + 2m(\tau + 1))\right] \quad . \tag{A2}$$

Calculating the optical depth, τ, requires numerically integrating

$$\tau_\lambda(s) = \int_0^s \alpha_\lambda \frac{\alpha_5'}{\alpha_5}\mathrm{d}s \quad , \tag{A3}$$

where α_5 is the absorption coefficient at the reference wavelength, 5000 Å, calculated by KORG, and α_5' is the absorption coefficient at the reference wavelength supplied by the model atmosphere. Their ratio is the correction factor to α_λ which enforces greater consistency between the model atmosphere and spectral synthesis. KORG computes τ_λ by evaluating the equivalent integral

$$\tau_\lambda(s) = \int_0^{\ln \tau_5'(s)} \tau_5' \frac{\alpha_\lambda}{\alpha_5}\mathrm{d}(\ln \tau_5') \quad , \tag{A4}$$

where τ_5' is the optical depth at the reference wavelength per the model atmosphere. This integral is numerically preferable, since atmospheric layers are spaced uniformly in $\ln \tau_5'$, and the integrand of A4 is more nearly linear than that of A3.